

Notes

Reactions of Bis(2-pyridyl)amine and Its Deprotonated Anion with Ruthenium and Osmium Carbonyl Complexes

Matti Haukka,* Philippe Da Costa, and Saija Luukkanen

University of Joensuu, Department of Chemistry, P.O. Box 111, FIN-80101 Joensuu, Finland

Received June 24, 2003

Summary: The reactions and coordination geometry of bis(2-pyridyl)amine (Hdpa) and its deprotonated anion (dpa) can be effectively modified by the reaction conditions. Depending on the solvent system, the reaction of multinuclear ruthenium carbonyls such as $Ru_3(CO)_{12}$ and $[Ru(CO)_3Cl_2]_2$ with Hdpa at moderate reaction temperatures lead to low yields of a monomeric *cis*(CO), *cis*(Cl)-Ru(Hdpa)(CO)₂Cl₂ or a dimeric metal–metal-bonded $[Ru(dpa)_2(CO)_2]_2$. In organic solvents high temperatures favor the formation of $[Ru(dpa)_2(CO)_2]_2$ from clustered $Ru_3(CO)_{12}$ and Hdpa. The high-temperature reactions in HCl solution can, in turn, be used for selective synthesis of *cis*(CO), *cis*(Cl)-Ru(Hdpa)(CO)₂Cl₂. dpa (deprotonated with CH_3Li) readily reacts with $[Ru(CO)_3Cl_2]_2$, $Ru_3(CO)_{12}$, or $H_4Ru_4(CO)_{12}$ in organic solvents, leading to $[Ru(dpa)_2(CO)_2]_2$. Under the corresponding conditions Os carbonyls produce a new type of dpa-bridged dimer compound without a direct metal–metal bond, $[Os(dpa)(CO)_2(CH_3)]_2$, in addition to the ruthenium dimer equivalent $[Os(dpa)_2(CO)_2]_2$.

Bis(2-pyridyl)amine (Hdpa) and its deprotonated anion (dpa) have been widely used as ligands in a variety of metal complexes. Hdpa is most commonly coordinated by both of its pyridyl nitrogens, forming chelating structures. In this coordination mode Hdpa is usually in the *trans,trans* configuration. The possible configurations of Hdpa and dpa are shown in Figure 1.

Several metals are known to have pyridyl-coordinated chelating complexes of Hdpa.^{1–14} Monodentate^{15,16} and

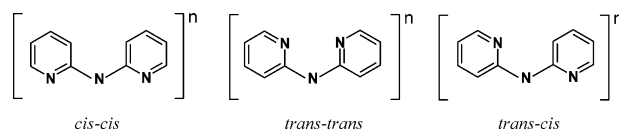


Figure 1. Configurations of Hdpa ($n = 0$) and dpa ($n = -1$). The amine hydrogens of Hdpa have been omitted for clarity.

ortho-metallated¹⁷ Hdpa complexes are less common but also known. In ortho-metallated $Ru_3(\mu-H)(\mu,\eta^3-Hdpa-C,N,N)(CO)_9$ one of the ruthenium centers is chelated by the aromatic nitrogens of Hdpa. Simultaneously, the *trans,trans*-configured Hdpa is attached to a neighboring ruthenium through a metallated carbon.

In comparison to Hdpa, the coordination modes of the dpa are more versatile. The anionic dpa is able to act as a tridentate, bidentate, or monodentate nitrogen ligand. Bridging or chelating coordination modes are typically the dominating ones. In a tridentate bridging coordination the bis(2-pyridyl)amide ligand usually has a *cis,cis* configuration (Figure 1).^{18–27} In a typical

(10) Madureira, J.; Santos, T. M.; Goodfellow, B. J.; Lucena, M.; Pedrosa de Jesus, J.; Santana-Marques, M. G.; Drew, M. G. B.; Felix, V. *J. Chem. Soc., Dalton Trans.* **2000**, 4422.

(11) Lescouezec, R.; Marinescu, G.; Munoz, M. C.; Luneau, D.; Andruh, M.; Lloret, F.; Faus, J.; Julve, M.; Mata, J. A.; Llusar, R.; Cano, J. *New J. Chem.* **2001**, 25, 1224.

(12) Akhter, P.; Fitzsimmons, P.; Hathaway B. *Acta Crystallogr., Sect. C* **1991**, C47, 308.

(13) Akhter, P.; Hathaway, B. *Acta Crystallogr.* **1991**, C47, 86.

(14) Howie, R. A.; Izquierdo, G.; McQuillan, G. P. *Inorg. Chim. Acta* **1983**, 72, 165.

(15) Howie, R. A.; McQuillan, G. P. *J. Chem. Soc., Dalton Trans.* **1986**, 759.

(16) Creaven, B. S.; Howie, R. A.; Long, C. *Acta Crystallogr., Sect. C* **2000**, 56, e181.

(17) Cabeza, J. A.; del Rio, I.; Garcia-Granda, S.; Riera, V.; Suarez, M. *Organometallics* **2002**, 21, 2540.

(18) Yang, E. C.; Cheng, M. C.; Tsai, M. S.; Peng, S. M. *J. Chem. Soc., Chem. Commun.* **1994**, 2377.

(19) Cotton, F. A.; Daniels, L. M.; Jordan, G. T.; Murillo, C. A. *J. Am. Chem. Soc.* **1997**, 119, 10377.

(20) Clérac, R.; Cotton, F. A.; Dunbar, K. R.; Murillo, C. A.; Pascual, I.; Wang, X. *Inorg. Chem.* **1999**, 38, 2655.

(21) Cotton, F. A. *Inorg. Chem.* **1998**, 37, 5710.

(22) Clérac, R.; Cotton, F. A.; Dunbar, K. R.; Lu, T.; Murillo, C. A.; Wang, X. *J. Am. Chem. Soc.* **2000**, 122, 2272.

(23) Clérac, R.; Cotton, F. A.; Daniels, L. M.; Dunbar, K. R.; Murillo, C. A.; Pascual, I. *Inorg. Chem.* **2000**, 39, 748.

(24) Sheu, J. T.; Lin, C. C.; Chao, I.; Wang, C. C.; Peng, S. M. *Chem. Commun.* **1996**, 315.

(25) Cotton, F. A.; Daniels, L. M.; Murillo, C. A.; Pascual, I. *Inorg. Chem. Commun.* **1998**, 1, 1.

* To whom correspondence should be addressed. Tel: 358-13-2513346. Fax: 358-13-2513344. E-mail: Matti.Haukka@joensuu.fi.

(1) Yan, B.; Yan, X.; Bu, X.; Goh, N. K.; Chia, L. S.; Stucky, G. D. *Dalton* **2001**, 2009.

(2) Coombs, T. D.; Brisdon, B. J.; Curtis, C. P.; Mahon, M. F.; Brewer, S. A.; Willis, C. R. *Polyhedron* **2001**, 20, 2935.

(3) Castillo, O.; Luque, A.; De la Pinta, N.; Roman, P. *Acta Crystallogr., Sect. E* **2001**, 57, m384.

(4) Zhu, H.; Strobele, M.; Yu, Z.; Wang, Z.; Meyer, H.-J.; You, X. *Inorg. Chem. Commun.* **2001**, 4, 577.

(5) Lu, J. Y.; Schroeder, T. J.; Babb, A. M.; Olmstead, M. *Polyhedron* **2001**, 20, 2445.

(6) Du, M.; Bu, X.-H.; Weng, L.-H.; Leng, X.-B.; Guo, Y.-M. *Acta Crystallogr., Sect. E* **2001**, 57, m25.

(7) Kumagai, H.; Kitagawa, S.; Maekawa, M.; Kawata, S.; Kiso, H.; Munakata, M. *Dalton* **2002**, 2390.

(8) Villanueva, M.; Mesa, J. L.; Urtiaga, M. K.; Cortes, R.; Lezama, L.; Arriortua, M. I.; Rojo, T. *Eur. J. Inorg. Chem.* **2001**, 1581.

(9) Freire, E.; Baggio, S.; Mombro, A.; Baggio, R. *Aust. J. Chem.* **2001**, 54, 193.

chelating system, one of the pyridyl nitrogens is attached, together with the amino nitrogen, to the same metal. The second pyridyl nitrogen then either is bonded to the adjacent metal center, which leads to a chelating-bridging coordination or is left dangling free. In chelating-bridging systems the *cis,cis* configuration of dpa is the most common,^{28–34} although in some aluminum compounds another type of chelating-bridging mode has been reported.^{35,36}

As in the case of Hdpa, a variety of bidentate pyridyl-coordinated *trans,trans*-configured complexes of dpa are also known.^{32,37–44} The *trans,cis* arrangement of the dpa is clearly less common than *trans,trans* or *cis,cis*, but this mode can also be found, for example, in polymeric $[(\text{CH}_3)_2\text{Ti}(\text{dpa})]_\infty$.³²

In our current research we have undertaken further study of the reactions of Hdpa and dpa with a series of carbonyl-containing Ru and Os compounds. Our primary aim was to investigate the effects of the reaction conditions on the reactivity of bis(2-pyridyl)amine and on the coordination modes of Hdpa and dpa ligands.

It has recently been reported that Hdpa can be coordinated to a ruthenium center via ortho metalation, leading to C,N,N-coordinated $\text{Ru}_3(\text{Hdpa})(\text{CO})_9$.¹⁷ In the corresponding reaction of Hdpa with the trinuclear osmium cluster no ortho metalation occurred but the amino group was deprotonated.¹⁷ The deprotonation was accompanied by the formation of a bidentate bridging coordination, where one of the aromatic nitrogens is bonded to one osmium center and the deprotonated amino nitrogen to the neighboring Os.¹⁷

We conducted the reaction of Hdpa with $\text{Ru}_3(\text{CO})_{12}$ in two steps. (1) The reactants were refluxed in a nonpolar solvent, *n*-hexane, to yield the primary solid product. (2) This primary product was then extracted with THF, and the final product was obtained by evaporating the solvent to dryness. This procedure

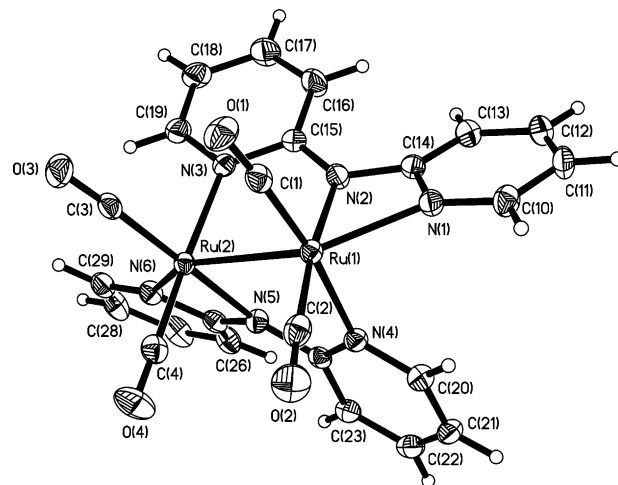


Figure 2. Molecular structure of $[\text{Ru}(\text{dpa})(\text{CO})_2]_2$ (**1**) and the numbering scheme for **1** and **2**. The thermal ellipsoids are drawn at the 50% probability level. Selected bond lengths (Å) and angles (deg): Ru(1)–Ru(2) = 2.6614(2), Ru(1)–N(1) = 2.221(2), Ru(1)–N(2) = 2.110(2), N(1)–C(14)–N(2) = 107.1(2), N(2)–C(15)–N(3) = 114.0(2), Os(1)–Os(2) = 2.6862(5), Os(1)–N(1) = 2.205(9), Os(1)–N(2) = 2.123(8), Os(2)–N(3) = 2.202(8), N(1)–Os(1)–N(2) = 105.4(8), N(2)–C(15)–N(3) = 116.0(9).

produced a low yield of a dimeric ruthenium compound, $[\text{Ru}(\text{dpa})(\text{CO})_2]_2$ (**1**), shown in Figure 2.⁵¹

The formation of $[\text{Ru}(\text{dpa})(\text{CO})_2]_2$ shows that deprotonation of Hdpa is also possible in reactions with ruthenium carbonyl clusters, even at relatively low temperatures. As a result of the chelating-bridging coordination mode, the dpa ligands in **1** are forced into a *cis,cis* arrangement. This closely resembles the coordination geometry found in $\text{V}_2(\text{dpa})_4$ ³³ and in $[(\text{CH}_3)_2\text{In}(\text{dpa})]_2$.³² In contrast to the $\text{V}_2(\text{dpa})_4$ and $[(\text{CH}_3)_2\text{In}(\text{dpa})]_2$ types of compounds, the metal–metal distance in $[\text{Ru}(\text{dpa})(\text{CO})_2]_2$ is relatively short, 2.6614(2) Å, indicating a clear bonding interaction between the two ruthenium centers. However, the Ru–Ru distance found in **1** is considerably longer than in trinuclear $\text{Ru}_3(\text{dpa})_4\text{Cl}_2$ (2.2573(5) Å), where delocalized three-centered $\text{Ru}^{\text{II}}\text{–Ru}^{\text{II}}\text{–Ru}^{\text{II}}$ bonding is reported to further strengthen the metal–metal interaction.²⁴

The yield of $[\text{Ru}(\text{dpa})(\text{CO})_2]_2$ could be improved by using an elevated temperature. When $\text{Ru}_3(\text{CO})_{12}$ was allowed to react with Hdpa in a tightly closed autoclave at 220 °C using toluene as solvent, $[\text{Ru}(\text{dpa})(\text{CO})_2]_2$ was obtained in ca. 55% yield. The same approach also worked well for $\text{Os}_3(\text{CO})_{12}$, the yield of $[\text{Os}(\text{dpa})(\text{CO})_2]_2$ (**2**) being ca. 65%.

The redox properties of **1** and **2** were compared in detail by cyclic voltammetry in DMSO/0.1 M TBAP (Figure 3). On a vitreous carbon electrode the CV of **1** (Figure 3 (–•–)) exhibits an irreversible broad cathodic wave at $E_{\text{p,c}} = -2.44 \text{ V}$ ⁵² and an irreversible wave at $E_{\text{p,a}} = 0.27 \text{ V}$. An exhaustive reduction at -2.45 V consumes only one electron per molecule of **1** and induces a dark orange solution, indicating formation of an oligomeric Ru^{I} species. However, by comparison of the intensities of both waves, **1** should be oxidized by a bielectronic process. With regard to the $[\text{Ru}^{\text{I}}(\text{bpy})(\text{CO})_2\text{–}(\text{CH}_3\text{CN})]_2^{2+}$ complex,⁴⁵ the oxidation process could lead to the formation of a Ru(II) monomer complex, which results from the oxidation-induced breakage of the $\text{Ru}^{\text{I}}\text{–}$

(26) Aduldecha, S.; Hathaway, B. *J. Chem. Soc., Dalton Trans.* **1991**, 993.

(27) Wu, L. P.; Field, P.; Morrissey, T.; Murphy, C.; Nagle, P.; Hathaway, B.; Simmons, C.; Thornton, P. *J. Chem. Soc., Dalton Trans.* **1990**, 3835.

(28) Deacon, G. B.; Faulks, S. J.; Gatehouse, B. M.; Jozsa, A. J. *Inorg. Chim. Acta* **1977**, 21, L1.

(29) Zhao, Q.; Sun, H.-S.; Chen, W.-Z.; Liu, Y.-J.; You, X.-Z. *J. Organomet. Chem.* **1998**, 556, 159.

(30) Tayebani, M.; Gambarotta, S.; Yap, G. *Organometallics* **1998**, 17, 3639.

(31) Liu, W.; Hassan, A.; Wang, S. *Organometallics* **1997**, 16, 4257.

(32) Gornitzka, H.; Stalke, D. *Eur. J. Inorg. Chem.* **1998**, 311.

(33) Cotton, F. A.; Daniels, L. M.; Murillo, C. A.; Zhou, H.-C. *Inorg. Chim. Acta* **2000**, 305, 69.

(34) Cotton, F. A.; Daniels, L. M.; Jordan, G. T., IV; Murillo, C. A.; Pascual, I. *Inorg. Chim. Acta* **2000**, 297, 6.

(35) Ashenhurst, J.; Brancalion, L.; Gao, S.; Liu, W.; Schmider, H.; Wang, S.; Wu, G.; Wu, Q. G. *Organometallics* **1998**, 17, 5334.

(36) Pfeiffer, M.; Baier, F.; Stey, T.; Leusser, D.; Stalke, D.; Engels, B.; Moigno, D.; Kiefer, W. *J. Mol. Model.* **2000**, 6, 299.

(37) Oro, L. A.; Ciriano, M. A.; Viguri, F.; Foces-Foces, C.; Cano, F. H. *Inorg. Chim. Acta* **1986**, 115, 65.

(38) Baxter, C. E.; Rodig, O. R.; Schlatter, R. K.; Sinn, E. *Inorg. Chem.* **1979**, 18, 1918.

(39) Freeman, H. C.; Snow, M. R. *Acta Crystallogr.* **1965**, 18, 843.

(40) Rodig, O. R.; Brueckner, T.; Hurlburt, B. K.; Schlatter, R. K.; Venable, T. L.; Sinn, A. *J. Chem. Soc., Dalton Trans.* **1981**, 196.

(41) Blake, A. J.; Parsons, S.; Rawson, J. M.; Winpenny, R. E. P. *Polyhedron* **1995**, 14, 1895.

(42) Cotton, F. A.; Daniels, L. M.; Jordan, G. T., IV; Murillo, C. A. *J. Am. Chem. Soc.* **1997**, 119, 10377.

(43) Wang, X.-M.; Sun, H.-S.; You, X.-Z.; Huang, X.-Y. *Polyhedron* **1996**, 15, 3543.

(44) Pfeiffer, M.; Murso, A.; Mahalakshmi, L.; Moigno, D.; Kiefer, W.; Stalke, D. *Eur. J. Inorg. Chem.* **2002**, 3222.

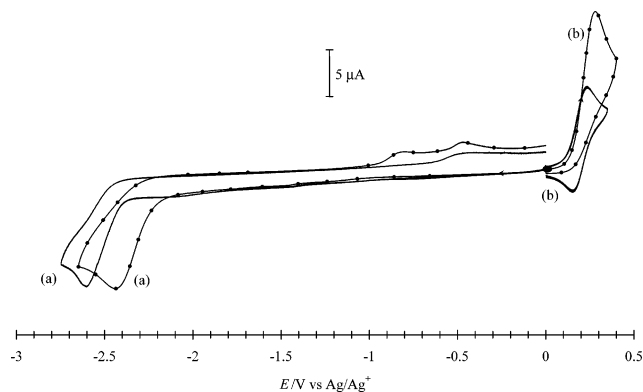


Figure 3. CVs (scan rate 100 mV s^{-1}) in DMSO/0.1 M TBAP on a VC electrode (diameter 3 mm): (—•—) 1.5 mM of **1** between (a) 0 and -2.65 V and (b) 0 and 0.40 V ; (—) 1.1 mM of **2** between (a) 0 and -2.75 V and (b) 0 and 0.35 V .

Ru^{I} bond and the coordination of solvent molecules. Despite the structural similarities of the dinuclear dpa carbonyl complexes $[\text{M}(\text{dpa})(\text{CO})_2]_2$ ($\text{M} = \text{Ru}, \text{Os}$), there are some differences in the electrochemical behavior of these compounds. The CV of **2** exhibits an irreversible two-electron cathodic peak at $E_{\text{p,c}} = -2.59 \text{ V}$ (Figure 3 (—•—)). An exhaustive reduction, carried out at -2.50 V , consumes two electrons per molecule of complex **2** and leads to a soluble orange product which, unlike in the case of **1**, is most probably a zerovalent oligomeric Os^0 species. In the positive potential region, a one-electron reversible wave ($E_{1/2} = 0.20 \text{ V}$, $I_{\text{p,a}}/I_{\text{p,c}} = 1$, $\Delta E_{\text{p}} = 0.09 \text{ V}$) (Figure 3 (— (b))) was obtained, formally corresponding to the $\text{Os}(\text{I})/\text{Os}(\text{II})$ redox couple of one of the two osmium metal centers. The reversibility of this system indicates that no $\text{Os}-\text{Os}$ bond cleavage occurred during the oxidation process. In addition, an irreversible system was observed at $E_{\text{p,a}} = 0.60 \text{ V}$, corresponding to the oxidation of the second Os^{I} metal center. This process can be associated with the breakage of the $\text{Os}-\text{Os}$ bond and the formation of a $\text{Os}(\text{II})$ monomer complex.

When the reaction between $\text{Ru}_3(\text{CO})_{12}$ and Hdpa was carried out in HCl solution at elevated temperature (200°C in an autoclave), the cluster core was completely broken and chlorinated mononuclear $\text{Ru}(\text{Hdpa})(\text{CO})_2\text{Cl}_2$ was obtained. The HCl reaction led mainly to the *cis*(CO),*cis*(Cl) isomer of $\text{Ru}(\text{Hdpa})(\text{CO})_2\text{Cl}_2$ (**3a**) shown in Figure 4. Only minor amounts of *cis*(CO),*trans*(Cl)- $[\text{Ru}(\text{Hdpa})(\text{CO})_2\text{Cl}_2]$ (**3b**) were found in some of the reaction products. The isomers are analogous to the corresponding 2,2'-bipyridine complexes of $\text{Ru}(\text{bpy})(\text{CO})_2\text{Cl}_2$ ⁴⁶ and could be identified by NMR.

It was also possible to obtain the *cis*(CO),*cis*(Cl) isomer of $\text{Ru}(\text{Hdpa})(\text{CO})_2\text{Cl}_2$ by refluxing $[\text{Ru}(\text{CO})_3\text{Cl}_2]_2$ and Hdpa in THF. However, although the selectivity of the *cis*(CO),*cis*(Cl) isomer was very good in this procedure, the total yield remained very low.

The *cis*(CO),*trans*(Cl) isomer of $\text{Ru}(\text{Hdpa})(\text{CO})_2\text{Cl}_2$ (**3b**) could be synthesized by allowing RuCl_3 to react with Hdpa in an alcohol solution under a CO atmosphere. The same method has been used previously, for example, in the synthesis of *cis*(CO),*trans*(Cl)- $\text{Ru}(\text{dmbpy})-$

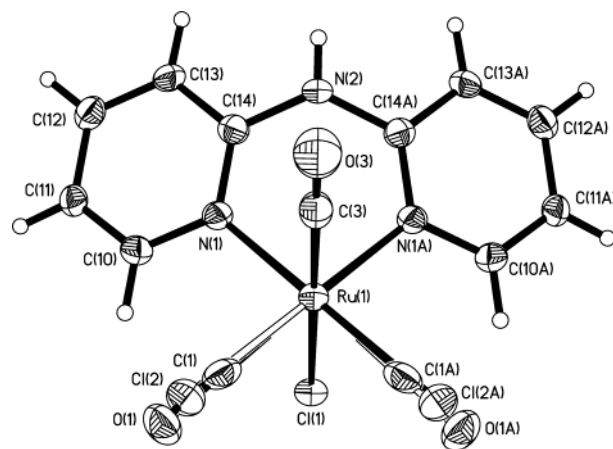


Figure 4. Molecular structure of *cis*(CO),*cis*(Cl)- $\text{Ru}(\text{Hdpa})-(\text{CO})_2\text{Cl}_2$ (**3a**). The thermal ellipsoids are drawn at the 50% probability level. Carbonyl and chloride ligands are located in two positions, owing to disorder. Selected bond lengths (\AA) and angles (deg): $\text{Ru}(1)-\text{N}(1) = 2.107(3)$, $\text{Ru}(1)-\text{Cl}(1) = 2.419(2)$, $\text{Ru}(1)-\text{C}(1) = \text{Ru}(1)-\text{Cl}(2) = 1.853(18)$, $\text{Ru}(1)-\text{C}(3) = 1.867(7)$, $\text{Cl}(1)-\text{Ru}(1)-\text{C}(3) = 178.4(2)$, $\text{N}(1)-\text{Ru}(1)-\text{N}(1\text{A}) = 86.0(2)$, $\text{C}(14)-\text{N}(2)-\text{C}(14\text{A}) = 126.1(5)$.

$(\text{CO})_2\text{Cl}_2$ (dmbpy = 4,4'-dimethyl-2,2'-bipyridine).⁴⁷ Even though **3b** was the major component, considerable amounts of **3a** were formed even in this reaction. The ratio of **3b/3a** was typically 2/1.

Although there are structural resemblances between $\text{Ru}(\text{Hdpa})(\text{CO})_2\text{Cl}_2$ and the corresponding 2,2'-bipyridine complex $\text{Ru}(\text{bpy})(\text{CO})_2\text{Cl}_2$, there are some distinct differences in the electrochemical behavior of these compounds. The one-electron reversible system corresponding to the $\text{Ru}(\text{II})/\text{Ru}(\text{III})$ redox couple observed for $\text{Ru}(\text{bpy})(\text{CO})_2\text{Cl}_2$ ⁴⁸ was not found for **3a**. Instead, an irreversible system at $E_{\text{p,a}} = 1.50 \text{ V}$ was the dominating feature of the CV of **3a**. This irreversibility indicates that the metal-center oxidation process may be associated with the amine oxidation. Indeed, under the same conditions, uncomplexed Hdpa has an irreversible oxidation peak at 1.00 V , which is thought to be associated with the amine of the ligand.^{49,50} In the negative potential area, **3a** exhibits an irreversible reduction peak at $E_{\text{p,c}} = -1.92 \text{ V}$. It has been well established that the two-electron reduction of *trans*(Cl)- or *cis*(Cl)- $\text{Ru}(\text{bpy})-(\text{CO})_2\text{Cl}_2$ leads to the formation of polymeric $[\text{Ru}(\text{bpy})(\text{CO})_2]_n$.⁴⁸ However, an exhaustive reduction of **3a** on a platinum sheet at -2.10 V consumes only about one electron per molecule of ruthenium complex and produces a soluble orange species, most probably due the formation of a dimeric Ru^{I} compound. When the exhaustive reduction was carried out in deuterated d_6 -DMSO and followed by ^1H NMR, the aromatic region revealed 13 overlapping patterns for 18 protons, which is notably different from that recorded for **3a** before reduction (7 overlapping patterns for 9 protons). The resonance of the Hdpa ligand protons, initially located between 10.9 and 7.2 ppm for **3a**, shifted toward high-

(47) Homanen, P.; Haukka, M.; Luukkanen, S.; Ahlgrén, M.; Pakkanen, T. A. *Eur. J. Inorg. Chem.* **1999**, 101.

(48) Chardon-Noblat, S.; Da Costa, P.; Deronzier, A.; Haukka, M.; Pakkanen, T. A.; Ziessel, R. *J. Electroanal. Chem.* **2000**, 490, 62.

(49) Morris, D. E.; Ohsawa, Y.; Segers, D. P.; DeArmond, M. K.; Hanck, K. W. *Inorg. Chem.* **1984**, 23, 3010.

(50) Ellis, C. D.; Margerum, L. D.; Murray, R. W.; Meyer, T. J. *Inorg. Chem.* **1983**, 22, 1283.

(45) Chardon-Noblat, S.; Cripps, G. H.; Deronzier, A.; Field, J. S.; Gouws, S.; Haines, R. J.; Southway, F. *Organometallics* **2001**, 20, 1668.

(46) Haukka, M.; Kiviaho, J.; Ahlgrén, M.; Pakkanen, T. A. *Organometallics* **1995**, 14, 825.

energy field conditions (~ -1.2 ppm). Such a shift reflects the increasing electronic density of the Hdpa subunit due to the one-electron reduction. Similar shifts have been previously observed also for the reduction of the related mononuclear $\text{Ru}^{\text{II}}\text{-bpy}$ to the dinuclear $\text{Ru}^{\text{I}}\text{-bpy}$.⁴⁵

When the deprotonated (with methyllithium at -70 °C) anionic dpa was allowed to react with the multinuclear ruthenium carbonyls $[\text{Ru}(\text{CO})_3\text{Cl}_2]_2$, $\text{Ru}_3(\text{CO})_{12}$, and $\text{H}_4\text{Ru}_4(\text{CO})_{12}$, the formation of the dimeric $[\text{Ru}(\text{dpa})(\text{CO})_2]_2$ was found to dominate the reactions. However, $[\text{Ru}(\text{dpa})(\text{CO})_2]_2$ was obtained with a reasonable yield only in the reaction between the nonclustered $[\text{Ru}(\text{CO})_3\text{Cl}_2]_2$ and dpa.

In a reaction between $[\text{Os}(\text{CO})_3\text{Cl}_2]_2$ and dpa under reflux in THF, a new type of product, $[\text{Os}(\text{dpa})(\text{CO})_2(\text{CH}_3)]_2$ (**4**), was slowly precipitated (Figure 5).

The crystal structure of **4** shows that there is no direct metal–metal bond, the Os–Os distance being 4.8633(3) Å. This is much longer than the true Os–Os bond distance of 2.6862(5) Å found in compound **2**. In $[\text{Os}(\text{dpa})(\text{CO})_2(\text{CH}_3)]_2$ the dpa ligands are again in a chelating–bridging mode, but the dpa is now in a trans,trans configuration and the aromatic nitrogens are bonded to the same metal center while the amine nitrogen is

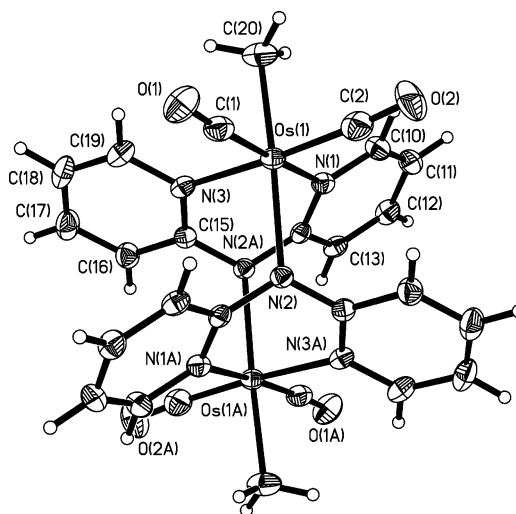


Figure 5. Molecular structure of $[\text{Os}(\text{dpa})(\text{CO})_2(\text{CH}_3)]_2$ (**4**). The thermal ellipsoids are drawn at the 50% probability level. Selected bond lengths (Å) and angles (deg): Os(1)··Os(2) = 4.8633(3), Os(1)–N(1) = 2.146(4), Os(1)–N(2) = 2.239(3), Os(1)–N(3) = 2.144(4), N(1)–Os(1)–N(3) = 82.81(13), N(3)–C(15)–N(2A) = 122.1(4), N(1)–C(14)–N(2A) = 123.6 (4).

bonded to the adjacent Os atom. Although $[\text{Os}(\text{dpa})(\text{CO})_2(\text{CH}_3)]_2$ was the predominant product, traces of $[\text{Os}(\text{dpa})(\text{CO})_2]_2$ were also observed in some reactions of $[\text{Os}(\text{CO})_3\text{Cl}_2]_2$. When the osmium carbonyl chloride reactant was replaced by the cluster compound $\text{Os}_3(\text{CO})_{12}$, the yield of $[\text{Os}(\text{dpa})(\text{CO})_2]_2$ was improved, but even in this case it remained very low and only a few crystals of **2** could be isolated.

Acknowledgment. Financial support in the form of a grant provided by the Academy of Finland is gratefully acknowledged.

Supporting Information Available: Text giving synthetic procedures, spectroscopic details, and electrochemical instrumentation and procedures and tables giving crystallographic data for **1**, **2**, **3a**, and **4**. This material is available free of charge via the Internet at <http://pubs.acs.org>.

OM030488N

(51) The X-ray diffraction data were collected on a Nonius KappaCCD diffractometer using Mo $K\alpha$ radiation ($\lambda = 0.71073$ Å). Crystallographic data for **1**: empirical formula, $\text{C}_{24}\text{H}_{16}\text{N}_6\text{O}_4\text{Ru}_2$; fw, 654.57; temperature (K), 150(2); crystal system, monoclinic; space group, $P2_1/n$; a (Å), 11.18300(10); b (Å), 12.37700(10); c (Å), 16.4926(2); γ (deg), 91.5590(6); V (Å³), 2281.93(4); Z , 4; r_{calcd} (Mg/m³), 1.905; μ (Mo $K\alpha$) (mm⁻¹), 1.37; $R1(I \geq 2\sigma)$, 0.0232; $wR2(I \geq 2\sigma)$, 0.0554. Crystallographic data for **2**: empirical formula, $\text{C}_{24}\text{H}_{16}\text{N}_6\text{O}_4\text{Os}_2$; fw, 832.83; temperature (K), 150(2); crystal system, monoclinic; space group, $P2_1/n$; a (Å), 11.1852(2); b (Å), 12.3410(3); c (Å), 16.4673(5); β (deg), 91.9150(10); V (Å³), 2271.82(10); Z , 4; r_{calcd} (Mg/m³), 2.435; μ (Mo $K\alpha$) (mm⁻¹), 11.222; $R1(I \geq 2\sigma)$, 0.0341; $wR2(I \geq 2\sigma)$, 0.0815. Crystallographic data for **3b**: empirical formula, $\text{C}_{12}\text{H}_9\text{Cl}_2\text{N}_3\text{O}_2\text{Ru}$; fw, 399.19; temperature (K), 120(2); crystal system, orthorhombic; space group, $Pnma$; a (Å), 7.5913(2); b (Å), 14.0646(4); c (Å), 12.6816(4); V (Å³), 1354.00(7); Z , 4; r_{calcd} (Mg/m³), 1.958; μ (Mo $K\alpha$) (mm⁻¹), 1.555; $R1(I \geq 2\sigma)$, 0.0334; $wR2(I \geq 2\sigma)$, 0.0725. Crystallographic data for **4**: empirical formula, $\text{C}_{26}\text{H}_{22}\text{N}_6\text{O}_4\text{Os}_2$; fw, 862.9; temperature (K), 150(2); crystal system, triclinic; space group, $P1$; a (Å), 8.0211(2); b (Å), 9.2464(2); c (Å), 9.8554(2); α (deg), 115.2540(10); β (deg), 96.8420(10); γ (deg), 104.3250(10); V (Å³), 619.11(2); Z , 1; r_{calcd} (Mg/m³), 2.314; μ (Mo $K\alpha$) (mm⁻¹), 10.299; $R1(I \geq 2\sigma)$, 0.0207; $wR2(I \geq 2\sigma)$, 0.0491. $R1 = \sum |F_o| - |F_c| / \sum |F_o|$. $wR2 = [\sum w(F_o^2 - F_c^2)^2 / \sum w(F_o^2)]^{1/2}$.

(52) All electrode potentials are referenced to 10 mM Ag/AgNO₃ in CH₃CN/0.1 M TBAP, which can be converted to the Fc/Fc⁺ couple by adding -0.05 V.